Springer

KSME

Journal of Mechanical Science and Technology 24 (10) (2010) 2075~2081
www.springerlink.com/content/1738-494x
DOI 10.1007/s12206-010-0703-z

Low-temperature creep behavior of ultrafine-grained 5083 Al alloy processed by equal-channel angular pressing †

Ho-Kyung Kim

Department of Automotive Engineering, Seoul National University of Technology, 172 Kongnung-dong, Nowon-ku, Seoul 139-743

(Manuscript Received October 12, 2009; Revised June 25, 2010; Accepted June 25, 2010)

Abstract

Low temperature creep behavior of ECAPed Al 5083 alloy with grain sizes of approximately 300 nm was investigated at temperatures of 498, 523 and 548 K. The value of the stress exponent was found to be 3.5 at a low stress level and increased to 5.0 at a high stress level. At the low stress level, the creep curve exhibits typical class II behavior due to the accumulated strain during the ECAP process, even though the creep is controlled by solute-drag processes with a stress exponent of 3.5. The average value of Q obtained from the analysis of the data is close to that for dislocation pipe diffusion. Therefore, on the basis of the activation energy in a temperature range of 498K to 548K at low and high stress level, the creep deformation is controlled by dislocation glide and climb processes, respectively, and the rate-controlling diffusion step might be dislocation pipe diffusion.

Keywords: ECAP; Creep; Activation energy; Ultra-fine grained microstructures

1. Introduction

The mechanical behavior of ultrafine grained (UFG) materials has attracted much attention in recent years, since these materials exhibit high tensile strength and hardness with fairly large ductility [1]. To produce materials with ultra-fine grain sizes, equal-channel angular pressing (ECAP) [2] has been adopted. The ECAP process is very effective in generating relatively bulk UFG aluminum [2], steels [3], and titanium [4]. The average grain sizes obtainable by the ECAP process are reported to fall in a range of 0.2 – 1ìm [2-4]. In ECAP, a billet is pressed through a die having two channels of equal cross section. The sample undergoes plastic deformation theoretically by pure shear when it passes through the intersecting corner. By pressing the same sample repetitively through the die, very high strain can be accumulated on the sample without change to its cross sectional area.

While there has been extensive research over the past decade on the creep deformation behavior of UFG metals and alloys, studies have mainly focused on superplasticity for Al alloys [5-7]. Tensile creep behavior of ECAPed UFG 5083 Al alloy was studied by Park et al. [6] in the temperature range of 498 - 548K and a strain range of 10 to 10^{-2} s^{-1}. They reported that low temperature superplasticity of the UFG 5083 Al alloy could be attributed to grain boundary sliding that is rate-controlled by grain boundary diffusion. The creep behavior of ECAPed Al and Al alloys, however, is still not fully understood. Tensile and compressive creep behavior of ECAPed pure Al was studied by Sklenicka et al. [8] from 423 - 523K and at applied stress levels ranging from 10 - 25 MPa. They reported that creep in the ECAPed Al occurred by lattice diffusion-controlled movement of dislocations, and that grain boundary sliding became increasingly important with an increase of the number of ECAP passes. However, these results were preliminary and provided limited information on the creep deformation mechanisms in ECAPed UFG Al alloys. The purpose of the present investigation is to examine the low temperature creep behavior of ECAPed UFG (d ≈ 300 nm) Al 5083 alloy.

2. Experimental procedures

A commercial 5083 Al alloy (Al–4.4Mg–0.7Mn–0.15Cr (in wt.%)) was supplied in the form of extruded bar. The alloy was annealed at 773K for 2 hours. ECAP of 8 passes (an effective strain of ~8) with route Bc was carried out at 473K on the annealed alloy. The average linear-intercept grain size of the as-ECAPed sample was about 0.3 μm. The detailed ECAP procedures and the microstructures of the sample have been described elsewhere [6].

All the creep tests were conducted using double-shear specimens from the ECAPed rods of 5083 Al alloy with a diame-

† This paper was recommended for publication in revised form by Associate Editor Seong Beom Lee

*Corresponding author. Tel.: +82 2 970 6348, Fax: +000
E-mail address: kimhk@snut.ac.kr

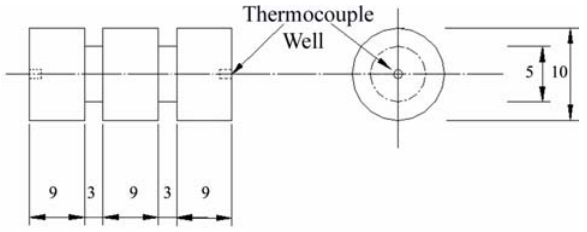

Fig. 1. Schematic of doublse-shear creep specimen geometry.

ter of 10 mm. The configuration and dimensions for the creep specimen are shown in Fig. 1. The creep tests were conducted in air in a three-zone furnace. The test temperature was monitored with chromel-alumel thermocouples held in contact with the specimen and was maintained within ±1K of the reported temperature. The strain during creep was measured with a linear variable differential transformer (LVDT), accurate to 1.7×10^{-3} mm. The LVDT signal was amplified, and monitored directly on a strip chart recorder. The shear stress, τ, and shear strain, γ, were converted to normal stress, σ, and normal strain, ε, using the expression $\sigma = 2\tau$ and $\varepsilon = 2/3\gamma$ [9]. The samples were tested under constant stresses at constant temperatures ranging from 498 to 548K corresponding to 0.58 to 0.65 T_m, where T_m is the incipient melting point.

3. Results and discussion

3.1 Creep curves

A large number of creep tests were conducted at stresses ranging from 10 to 100 MPa. All of the creep curves obtained in the present study exhibited only one type, regardless of stress levels. As shown in Fig. 2(a), the shape of the creep curve was typical class II (Metal type) behavior [10]: there is a normal primary creep stage, during which the creep rate decreases continuously with increasing time; this stage is then followed by a well-defined steady state period for which the creep rate remains essentially constant. This type of creep curve is clearly illustrated by the plots shown in Fig. 2(b) of the logarithmic strain rate $\dot{\varepsilon}$ against the total strain ε for tests conducted at different temperatures under the same stress. At a stress of 20 MPa, the normal primary stage extends to higher strain.

3.2 Stress dependence of the steady state creep rate

The results from a number of tests conducted at three different temperatures are shown in Fig. 3 in terms of steady state creep rate, $\dot{\varepsilon}$, against the true stress, σ, on a logarithmic scale. The creep data for coarse grained (CG) unECAPed 5083 Al alloy at 548K also are included in order to show the effect of grain size on creep strain rate. The average grain size of the unECAPed sample was 48 μm. For the ECAPed samples, the data show that the value of the stress exponent, n ($=\partial \ln \dot{\varepsilon} / \partial \ln \sigma$), was independent of temperature and that there is a significant variation in the stress exponent with stress level. The value of the stress exponent was found to be 3.5 ± 0.2 at a low

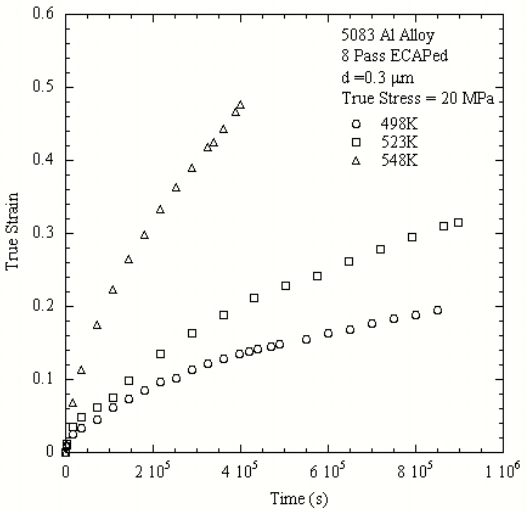

(a)

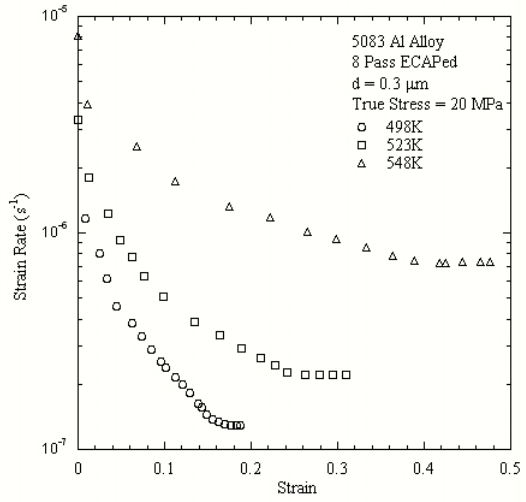

(b)

Fig. 2. Creep curves for 8 pass ECAPed 5083 Al alloy at 20 MPa: (a) strain against time, and (b) creep rate against strain.

stress level and increased up to 5.0 ± 0.2 at a high stress level. The stress exponents of 3.5 and 5.0 suggest that the creep of 5083 Al alloy is controlled by a dislocation glide process and by a dislocation climb process at low and high stress levels, respectively. There is no data available on the stress exponent for the low stress level of a similar alloy system at a similar testing temperature. However, some experimental data have been reported on stress exponents of similar alloy systems at strain rates ranging from 10^{-6} - 10^{-3}, corresponding to a high stress level at similar testing temperature. The value of the stress exponent 5.0 is in good agreement with the value of ~5 reported by Park et al. for the same ECAPed 5083 Al alloy at a strain rate of close to 10^{-4} at 498 to 548K [6]. However, they reported stress exponents of 5, 2.5, and 10 at high strain rate at a narrow strain region of one order of magnitude, in contrast to the present result of 5.0 at a wide range of strain rates from 10^{-6} - 10^{-3}. Hsiao and Huang reported a value of ~4 for 5083

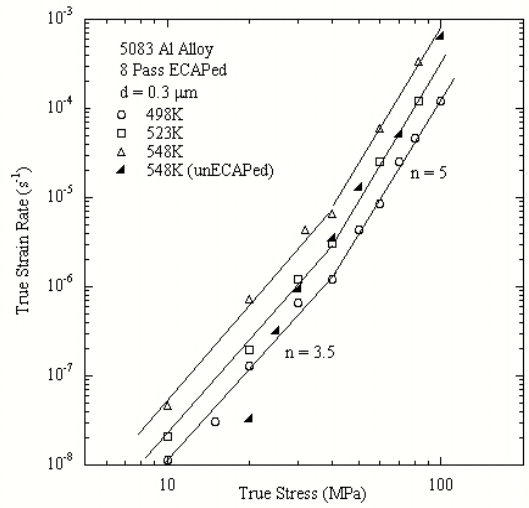

Fig. 3. Steady-state strain rate against stress for specimens tested from 498 to 548K.

Al alloy at strain rates ranging from 10^{-4} - 10^{-2} in a temperature range 423 to 523K [7]. Kawazoe et al. reported a value of 3.3 for ECAPed 5056 Al alloy at strain rates ranging from 10^{-5} - 10^{-4} in a temperature range of 498 to 523K [11]. For coarse unECAPed samples, the creep strain rates are much lower than those of ECAPed UFG samples. This behavior is partially due to the ECAPed sample undergoing high dislocation density produced strain during ECAP. The stress exponent of the unECAPed samples does not remain constant but decreases with increasing applied stress. This behavior is similar to the observed deformation in DS (dispersion strengthened) alloys and Al alloys prepared by powder metallurgy [13], and can be interpreted in terms of a threshold stress. It is well known that a threshold stress may arise from the interaction between lattice dislocations that move by viscous glide in the interiors of grains providing obstacles to boundary sliding, and dispersion particles that are present in the interiors of the blocking grains [14].

3.3 Threshold stress

To estimate the values of the threshold stresses associated with the creep of 5083 Al alloy, the data at a single temperature were plotted as $\dot{\varepsilon}^{1/n}$ against ó on a double linear scale. The datum points of this plot were best fitted on a straight line by varying the n values. The n values were taken as 2, 3, 4, 5, and 7. For ECAPed UFG samples, a stress exponent of 4 yielded the best linear fit between $\dot{\varepsilon}^{1/n}$ and ó. The estimated values of $ó_{th}$ for ECAPed UFG samples were 3.7, 2.6, and 2.2 MPa for 498, 523, and 548K, respectively, as shown in Fig. 4(a). For unECAPed samples, a stress exponent of 5 yielded the best linear fit between $\dot{\varepsilon}^{1/n}$ and ó. The value of $ó_{th}$ for unECAPed samples at 548K was 5.4 MPa, as shown in Fig. 4(b). It is reported that the threshold stress of a modified 5083 Al alloy has values of 20.1 MPa and 13.3 MPa at 523K and 573K, respectively. For the cryomilled UFG 5083 Al alloy,

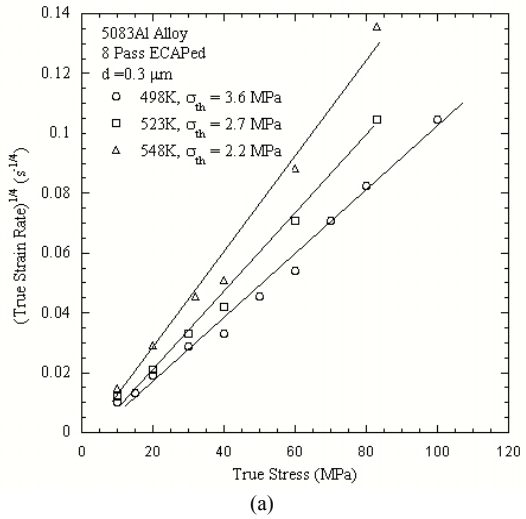

Fig. 4. Determination of the threshold stress by plotting $\dot{\varepsilon}^{1/n}$ against σ on (a) ECAPed UFG alloy and (b) unECAPed CG alloy.

the threshold value ranged from 11.6 MPa to 8.5 MPa at 573K to 648K [13]. The authors speculated that nano-scale dispersion particles, which are introduced into 5083 Al during cryomilling, exist in the interiors of the grains of cryomilled 5083 Al. These impurities may segregate to the grain boundaries, leading to a threshold stress for sliding. It is well known that the threshold stress increases with decreasing temperature [14]. The present value of 5.4 MPa at 548K is lower than that of cryomilled 5083 Al at higher temperatures [13], indicating that the binding stress between the dislocations and the particles of the cryomilled 5083 Al sample is higher, compared to the present unECAPed 5083 Al alloy.

At present, it is not clear why the present ECAPed UFG 5083 Al alloy shows a negligible threshold stress. The very low threshold stress in the present ECAPed UFG 5083 Al alloy can be explained by the following assumption. The threshold stress is known to increase with increasing grain size [15]. The present findings on temperature and grain size de-

pendencies of threshold stress are in good agreement with the previously reported data [14]. The threshold stress is related to initiation of glide at triple junctions, ledges, or particles at the grain boundaries, and not diffusion. However, diffusion and recovery effects can reduce this strength via thermal activation. As the temperature increases, thermal vibration of pinned dislocations enhances their mobility. These dislocations can then overcome obstacles more easily to initiate the glide process. Microstructures with smaller grain sizes have more grain corners as well as particles per unit volume lying on grain boundaries [14]. Thus, more glide sources are activated in fine grain metals, resulting in a greater creep strain in comparison with coarse grain metals. This leads to lower threshold stress in the UFG 5083 Al alloy.

3.4 Activation energy for creep

The activation energy for creep can be determined using the power-law creep equation

$$\dot{\varepsilon} = A(\sigma - \sigma_{th})^n \exp(-\frac{Q}{RT}) \quad (1)$$

where $\dot{\varepsilon}$ is the steady state creep rate, σ_{th} the threshold stress, n the stress exponent, and A a material constant. Q the activation energy, R the gas constant, and T the absolute temperature. For calculating the activation energy for the creep, the data of Fig. 3 were used to plot the logarithmic $\dot{\varepsilon}\, G^{n-1} T$ against 1000/T at low ($\sigma - \sigma_{th}$ = 30 MPa) and at high stress ($\sigma - \sigma_{th}$ = 80 MPa). The activation energy was then determined from the slope of the resultant straight line, which, according to well-documented analysis [16], is equal to $-2.3R \times d(\log \dot{\varepsilon})/(d(1/T))$. In estimating Q from the method, information concerning the shear modulus, G, was taken from the data available on pure Al [17]. The modulus G for Al is expressed as 3.022×10^4 - 16T (MPa). The values of Q obtained from the analysis of the data are 72.6 kJ/mole and 96.1 kJ/mole at low and high stress levels, respectively. The value of Q (= 72.6 kJ/mole), as shown in Fig. 5(a), is slightly lower than that for grain boundary diffusion Q_{gb} of Al (= 86 kJ/mole) [18]. The value of Q is much lower than that for Mg diffusion in Al (= 130.5 kJ/mole) [18]. Recently, Kolobov et al. reported that the Q_{gb} value of ECAPed Ni was much lower than that of coarse grained Ni due to the nonequilibrium nature of grain boundaries induced by severe plastic deformation [12]. In addition, the activation energy Q is generally equal to that for dislocation pipe diffusion (Q_p) and $Q = 2/3Q_L$ from about 0.4 to 0.6 T_m [16]. The lattice diffusion Q_L is reported to be 142kJ/mole [18]. The test temperatures employed in the present study for 5083 Al alloy were in a range of 0.58 to 0.65 T_m and the measured Q value (Q/Q_L =0.51) is consistent with results reported in the literature [16]. It is thus suggested that, at a low stress level, the creep of 5083 Al alloy is controlled by a dislocation glide process, and the rate-controlling diffusion step may be dislocation pipe diffusion or grain boundary diffusion. However, the stress exponent of 3.5 is not consistent

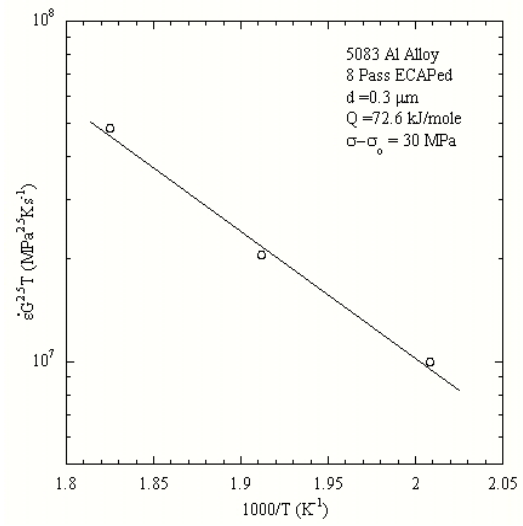

Fig. 5. Determination of the activation energy for creep in ECAPed UFG 5083 Al alloy (a) at low stress and (b) at high stress by plotting $\dot{\varepsilon}\, G^{n-1} T$ against 1000/T.

with the occurrence of grain boundary diffusion. Thus, on the basis of the activation energy of 72.6 kJ/mole and a stress exponent of 3.5 at low stress level, the creep deformation is controlled by a dislocation climb process, and the rate-controlling diffusion step might be dislocation pipe diffusion of the Mg atom in Al rather than grain boundary diffusion.

The value of Q obtained at high stress ($\sigma - \sigma_{th}$ = 80 MPa) is 96.1 kJ/mole, as shown in Fig. 5(b). This is higher than the value of 61 kJ/mole reported for the same ECAPed 5083 Al alloy at a strain rate of close to 5×10^{-4} at 498K to 548K [6]. The value of Q = 96.1 kJ/mole agrees with that for the activation energy for grain boundary diffusion Q_{gb} of Al (86 kJ/mole) [18] and is close to the value of dislocation pipe diffusion (Q/Q_L =0.68). On the basis of the activation energy in a temperature range of 498K to 548K at high stress level, the creep deformation is controlled by a dislocation climb process.

The rate-controlling diffusion step might be dislocation pipe diffusion of Al atom in Al rather than grain boundary diffusion since the stress exponents of 5 is not consistent with the occurrence of grain boundary diffusion.

3.5 Creep mechanisms

It is well known that the typical creep curve for class I (Alloy type) with a stress exponent of 3.5 shows little or no instantaneous strain upon application of the load, a brief period of either primary creep or inverted primary creep, and then steady state strain rates when the value of the stress exponent is approximately three. At present, it is not clear why, with a stress exponent of 3.5 at a low stress level, the creep curve exhibits typical class II (Metal type) behavior. This behavior can be explained by this assumption. If creep is controlled by solute-drag processes with a stress exponent of 3.5, then the creep rate at any instant is determined by the number of moving dislocations and their average velocity according to the equation, $\dot{\varepsilon} = \rho b \bar{v}$. If strain is accumulated through the ECAP process, the initial creep rate should then increase with increasingly accumulated strain levels, since progressively higher dislocation densities are present before creep starts. Even when glide processes govern the creep behavior, recovery processes tend to reduce the dislocation density towards the equilibrium levels for the applied stress. The creep rate of specimens with substantial accumulated strain then decreases as creep continues. Therefore, at a low stress level, the creep curve exhibits typical class II behavior due to the strain accumulated during the ECAP process, even though the creep is controlled by solute-drag processes with a stress exponent of 3.5.

To check this conclusion on solute-drag processes and dislocation climb mechanisms at a low and high stress levels, respectively, it is necessary to compare the experimental and theoretical creep rates. In class I or Alloy type creep with a stress exponent of 3.5, dislocations are understood to glide in a viscous manner due to their interaction with solute atoms. Several different drag processes have been proposed [19-21]. Among these mechanisms, calculations show that the major force retarding the glide of dislocations often arises from the presence of impurity atmospheres. In the theory of Weertman [19], it is assumed that the motion of dislocations occurs as sequential glide and climb processes, and the slower of these two processes is the rate-controlling mechanism. In the solid solution alloys when glide is slower than climb, the steady-state creep rate is given by

$$\dot{\varepsilon} = \frac{0.35}{e^2 c}\left(\frac{kT}{Gb^3}\right)^2\left(\frac{\bar{D}Gb}{kT}\right)\left(\frac{\sigma}{G}\right)^3 \tag{2}$$

where e is the solute-solvent size factor, c the solute concentration, k Boltzmann's constant (=1.38×10^{-23} J/K), b Burgers, $\bar{D}$ the chemical interdiffusivity of the solute atoms. On the other hand, the theory of Takeuchi and Argon [20] is based on

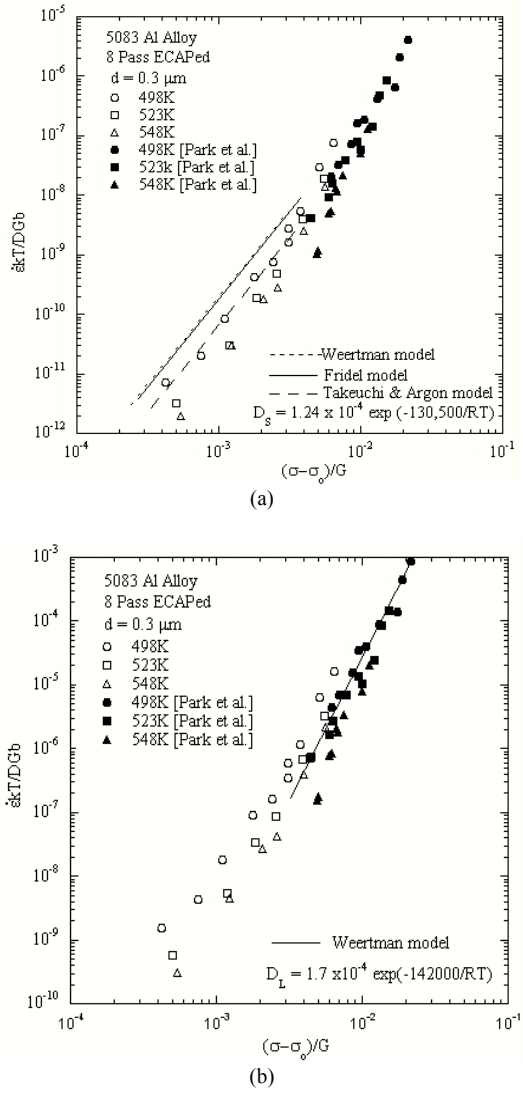

Fig. 6. Normalized strain rate against normalized stress for temperature from 498 to 548K: (a) solute drag creep and (b)D_L-controlled dislocation climb creep.

Cottrell-Jaswan interaction. By considering the rates of dislocation multiplication and annihilation, the steady-state creep rate due to dislocation glide is given by

$$\dot{\varepsilon} = \frac{0.125}{e^2 c}\left(\frac{kT}{Gb^3}\right)^2\left(\frac{\bar{D}Gb}{kT}\right)\left(\frac{\sigma}{G}\right)^3 \tag{3}$$

In the theory of Fridel [21], it is assumed that the diffusion of solute atoms is assisted by the line tension of the dislocations. The steady-state creep rate is given by

$$\dot{\varepsilon} = 0.18\left(\frac{\bar{D}Gb}{kT}\right)\left(\frac{\sigma}{G}\right)^3 \tag{4}$$

To evaluate the prediction of these glide models, the datum points shown in Fig. 3 were replotted in logarithmic form of

$\bar{D}$ kT/Gb against σ/G, putting e = 0.12, b = 2.86×10^{-10} m [18], the solute (=magnesium) concentration c = 0.049, G = 3.022 $\times10^{4}$ - 16T (MPa) [17], and taking $\bar{D}$ as the chemical inter-diffusivity of magnesium in aluminum; $\bar{D}$ = 1.24 x 10^{-4} exp (-130,500/RT) m^2s^{-1} [18]. The effect of solid solution of chromium and manganese, which are minor alloys addition to Al-Mg-Mn-Cr system alloys, is neglected for the sake of simplicity plots. Fig. 6(a) shows the predicted creep rates for the theories of Weertman [19], Takeuchi and Argon [20], and Fridel [21]. The experimental data reported by Park et al. [6] for ECAPed 5083 Al alloy obtained from strain rate change tests are also presented here. The results show that all of the experimental points now lie on a single line with a slope of about 3 at a low stress level. Within the region where n = 3.5, the present results are in better agreement with the prediction of the Takeuchi and Argon model [20], suggesting that dislocations glide in a viscous manner due to their interaction with solute atoms at a low stress level. However, there is another deformation mechanism of dislocation climb at $\sigma/G > 5\ x10^{-3}$.

According to the theoretical model for dislocation climb developed by Weertman [22], the steady state creep rate is given by

$$\dot{\varepsilon} = \alpha(\frac{D_L}{b^{3.5}M^{0.5}})(\frac{G\Omega}{kT})(\frac{\sigma}{G})^{4.5} \quad (5)$$

where α is a constant having a value in the range $0.015 < \alpha < 0.33$, D_L is the coefficient for lattice self-diffusion (=1.7 $x10^{-4}$ exp(-142000/RT) [18], Ω is the atomic volume, M is the number of dislocation sources per unit volume and is equivalent to 0.27 $\rho^{1.5}$. Dislocation density ρ is usually between 10^{10} and $10^{12}/m^2$. The creep rates were calculated from Eq. (5) and plotted in Fig. 6(b), taking α =0.1, M = 2.8 x $10^{17}/m^2$, and Ω = 1.66 x $10^{29}m^3$. Fig. 6(b) shows that the predicted creep rates by the Weertman model [22] are in better agreement with the experimental results, including the results by Park et al [6], suggesting that dislocation climb is the rate-controlling process at a high stress level.

The temperature compensation through D_L or D_S and G was not sufficient to make a good fit of the present experimental data due to the exact values of the diffusivity. And, microstructural evolution can partially affect the creep behavior. To check whether there was grain growth during creep deformation of the UFG 5083 Al alloy, it was found that there was a rapid decrease in microhardness of the ECAPed 5083 Al alloy at the beginning of annealing at 498K, suggesting that a significant grain growth of the alloy occurred. Thus, it can be predicted that microstructural evolution occurs during creep deformation.

3.6 Transitions between the creep mechanisms

There have been several experimental investigations of solid solution alloys to examine the deviation at high stress from viscous glide behavior with n ~3. For example, Yavari and Langdon [23] showed that there was marked change in the creep behavior of Al-Mg alloys with increasing stress such that there was an increase in the stress exponent from 3 to 4.5 and this change was due to the break-away of dislocations from their solute atmospheres. Also, it was demonstrated that for various solid solution alloys, the values of the experimental stresses marking the transitions from viscous glide to a break-away condition were in very good agreement with the stresses predicted by a break-away relationship developed by Fridel [21]. Following Fridel, the break-away stress, σ_c, which is necessary to break a dislocation from its solute atmosphere, may be expressed as

$$\sigma_c = (\frac{W_m^{\,2}c}{5kTb^3}) \quad (6)$$

where W_m is the binding energy between a solute atom and an dislocation, and c is the solute concentration. The value of W_m may be calculated from the theoretical expression [21]

$$W_m = -\frac{1}{2\pi}(\frac{1+\nu}{1-\nu})G|\Delta V_a| \quad (7)$$

where ΔV_a is the difference in volume between the solute and solvent atom, ν Poisson's ratio. For magnesium in aluminum, ΔV_a = 5.8 x 10^{-30} m^3 [24]. The estimated values σ_c are 46.7, 43.2, and 40.0 MPa for T = 498, 523, and 548 K, respectively. In practice, the experimental transitions occur at stresses of approximately 40 MPa for the testing temperatures, as shown in Fig. 3, and these values are very close to the estimated values from Eq. (6). Thus, it is concluded that the dislocations have broken away from their solute atom atmospheres at the transitions.

4. Conclusions

The creep behavior of well-annealed coarse-grained (CG) and ultrafine-grained (UFG) 5083 Al alloy at 498K, 523K, and 548K was investigated. For coarse unECAPed samples, the creep strain rates are much lower than those of ECAPed UFG samples. The value of the stress exponent was found to be 3.5 ± 0.2 at a low stress level and increased up to 5.0 ± 0.2 at a high stress level. At low stress level, the creep curve exhibits typical class II behavior due to the strain accumulated during the ECAP process, even though the creep is controlled by solute-drag processes with a stress exponent of 3.5. The average value of Q obtained from the analysis of the data is 72.6 kJ/mole and 96.1 kJ/mole at low and high stress levels, respectively. Therefore, on the basis of the activation energy and the stress exponent, it is concluded that at low stress level, the creep deformation is controlled by a dislocation glide process, and the rate-controlling diffusion step might be dislocation pipe diffusion of the Mg atom in Al rather than grain boundary diffusion. At high stress level, the creep deformation is controlled by a dislocation climb process, and the rate-

controlling diffusion step might be dislocation pipe diffusion of Al atom in Al.

References

[1] R. Z. Valiev, E. V. Kozlov, Y. F. Ivanov, J. Lian, A. A. Nazarov and B. Baudelet, Deformation behaviour of ultra-fine-grained copper, *Acta Metall. Mater.,* 42 (1994) 2467-2475.

[2] Y. Iwahashi, M. Furukawa, Z. Horita, M. Nemoto and T. G. Langdon, Microstructural characteristics of ultrafine-grained aluminum produced using equal-channel angular pressing., *Metal Mater., Trans.* 29A (1998) 2245-2252.

[3] D. H. Shin, W. J. Kim and W. Y. Choo, Grain refinement of a commercial 0.15%C steel by equal-channel angular pressing, *Scripta Mater.,* 41 (1999) 259-262.

[4] V. V. Stolyarov, Y. T. Zhu, I. V. Alexandrov, T. C. Lowe and R. Z. Valiev, Influence of ECAP routes on the microstructure and properties of pure Ti, *Mat. Sci. Eng*., A299 (2001) 59-67.

[5] I. Charit and R. S. Mishira, Low temperature superplasticity in a friction-stir-processed ultrafine grained Al–Zn–Mg–Sc alloy, *Acta Mater.,* 53 (2005) 4211-4223.

[6] K. T. Park, D. Y. Hwang, S. Y. Chang and D. H. Shin, Low-temperature superplastic behavior of a submicrometer-grained 5083 Al alloy fabricated by severe plastic deformation, *Metal Mater. Trans.,* 33A (2002) 2859.

[7] I. C. Hsiao and J. C. Huang, Deformation mechanisms during low-and high-temperature superplasticity in 5083 Al-Mg alloy, *Metal Mater. Trans*., 33A (2002) 1373-1384.

[8] V. Sklenicka, J. Dvorak, P. Kral, Z. Stonawska and M. Svoboda, Creep processes in pure aluminium processed by equal-channel angular pressing, *Mater. Sci. Eng.*, A410-411 (2005) 408-412.

[9] K. Isshiki, Z. Horita, T. Fujinami, T. Sano, M. Nemoto, Y. Ma and T. G. Langdon, A new miniature mechanical testing procedure: Application to intermetallics, *Metal Mater. Trans.,* 28A (1997) 2577-2582.

[10] W. R. Cannon and O. D. Sherby, High temperature creep behavior of class I and class II solid-solution alloys. *Metall. Trans*., 1 (1970) 1030-1032.

[11] M. Kawazoe, T. Shibata, T. Mukai and K. Higashi, Elevated temperature mechanical properties of A 5056 Al-Mg alloy processed by equal-channel-angular-extrusion, *Scripta Mater.*, 36 (1997) 699-705.

[12] Y. R. Kolobov, G. P. Garbovetskaya, M. B. Ivanov, A. P. Zhilyaev and R. Z. Valiev, Grain boundary diffusion characteristics of nanostructured nickel, *Scripta Mater.*, 44 (2001) 873-878.

[13] M. Chauhan, I. Roy and F. A. Mohamed, Creep behavior in near-nanostructured Al 5083 alloy, *Mater. Sc.i Eng.*, A410-411 (2005) 24-27.

[14] Y. Xun and F. A. Mohamed, Superplastic behavior of Zn-22%Al containing nano-scale dispersion particles, *Acta Mater.*, 52 (2004) 4401-4412.

[15] D. H. Bae and A. K. Ghosh, Grain size and temperature dependence of superplastic deformation in an Al-Mg alloy under isostructural condition, *Acta Mater.*, 48 (2000) 1207-124.

[16] S. L. Robinson and O. D. Sherby, Mechanical behavior of polycrystalline tungsten at elevated temperature, *Acta Metall.*, 17 (1969) 109-125.

[17] P. Yavari, F. A. Mohamed and T. G. Langdon, Creep and substructure formation in an Al-5% Mg solid solution alloy. *Acta Metall.*, 29 (1981) 1495-1507.

[18] H. J. Frost and M. F. Ashby Deformation-Mechanism Maps, Pergamon Press Oxford (1982) 1.

[19] J. Weertman, Steady-state creep of crystals., *J. Appl. Phys*., 28 (1957) 1185-1189.

[20] S. Takeuchi and A. S. Argon, Steady-state creep of alloys due to viscous motion of dislocations, *Acta Metall.,* 24 (1976) 883-889.

[21] J. Friedel, Dislocations, Pergamon Press, Oxford, 1964.

[22] J. Weertman, High temperature creep produced by dislocation motion, in J.E. Dorn memorial Symposium, Cleveland, Ohio, 1972.

[23] S. S. Vagarali and T. G. Langdon, Deformation mechanisms in h.c.p. metals at elevated temperatures—II. Creep behavior of a Mg-0.8% Al solid solution alloy, *Acta Metall.*, 30 (1982) 1157-1170.

[24] H. W. King, Quantitative size-factors for metallic solid solutions, *J. Mater. Sci.*, 1 (1966) 79-90.

Ho-Kyung Kim is a Professor of Department of Automotive Engineering of Seoul National University of Technology, Korea. He worked for Hyundai Aerospace Company as researcher. He received a B.S. in Mechanical Engineering from Hong-Ik University, Korea in 1982. He got MS and Ph.D. degrees from University of California at Irvine in U.S.A. His research areas include creep, fatigue and strength of structural materials.